Title	The effect of Single-Dose Spinal SRS On Ultrasound Propagation Velocity In Porcine Vertebral Bone

Topics/Areas:	Biomedical Engineering and Technology
Presentation format:	Paper
Name(s) of the author(s):	Julie E. Pollard*, Jessica Steinmann-Hermsen*, Paul M. Medin**, and Edmond Richer*
Department(s) and Affiliation(s):	* Southern Methodist University, Department of Mechanical Engineering ** UT Southwestern Medical Center at Dallas, Department of Radiology Oncology
Mailing Address(es):	*3101 Dyer Street, Suite 200 Dallas, TX 75205
E-mail Address(es):	richer@lyle.smu.edu
Contacts/Phone Number(s):	(214) 768-3059
Fax number(s):	(214) 768-1473
Corresponding author if different from lead author:	Edmond Richer; richer@lyle.smu.edu

Abstract/ Proposal:

The Effect of Single-Dose Spinal SRS On Ultrasound Propagation Velocity In Porcine Vertebral Bone

Julie E. Pollard, Jessica Steinmann-Hermsen, Paul M. Medin, and Edmond Richer

***Abstract*—Clinical radiation dose prescriptions for spinal radiosurgery have been escalated to levels currently accepted in intracranial radiosurgery with the expectation of increasing the durability of tumor control in the spinal column and reducing tumor induced paralysis and pain. Nevertheless, the maximum single-dose radiation treatment a vertebra can tolerate without loss of structural integrity is still unknown and may be exceeded in current prescriptions. The recent increase in dosage has correlated with a rise in late onset vertebral fractures. In this study four Yucatan Minipigs were administered 16 Gy or 18 Gy of radiation using stereotactic radiosurgery (SRS) from their fourth to their seventh cervical vertebra, parallel with the spine and focused on half of the vertebral body. One year after SRS, samples of the irradiated and non-radiated vertebrae were obtained and ultrasound propagation velocity, an indicator of bone elasticity, was measured in the axial and transverse directions. The results show a marked decrease in the ultrasound velocity as well as in the estimated elastic modulus in the radiated samples. Ultrasound propagation velocity and elastic modulus may be effective indicators of bone toxicity following irradiation.**

***Index Terms*—Bone, Ultrasound, Stereotactic Radiosurgery**

I. Introduction

VERTEBRAL metastases, from lung, breast, prostate, renal and myeloma malignancies, occur in over 100,000 individuals each year in the United States [1], [2]. Growing vertebral tumors cause loss of sensory and motor skills, debilitating pain, and vertebral collapse. External beam radiation therapy (plus steroids) has been proven effective for palliation of skeletal metastases providing pain relief with minimal morbidity.

In recent years, in an attempt to reduce treatment time and frequency, many investigators have pursued the use of image-guided stereotactic radiosurgery (SRS) to escalate single-fraction doses (> 8 Gy) to spinal metastases. Clinical results showed impressive durable pain responses (approximately 90%) and high rates of local control (approximately 80% or greater) [3], [4]. Improved local control combined with surgery and radiation lead to increased survival in patients with spinal cord compression from metastasis [5], [6]. The remarkable success of spinal SRS can be attributed to the accuracy of image-guided radiation delivery of high doses while surrounding tissue, including adjacent vertebrae, is relatively spared. Moreover, SRS is convenient and efficient because radiation is delivered on an outpatient basis in a single treatment. Traditionally, radiation has increased the risk of bone fracture only slightly [7], but increased fracture rates have been observed in stereotactic lung cancer irradiation (24–37 Gy in 1–5 fractions) [8], [9]. In breast and lung irradiation, bones in close proximity to the targeted cancer unavoidably receive some dose but standard practice is to minimize the dose to healthy tissue. In contrast, vertebrae are intentionally irradiated to extremely high doses in spinal SRS to control bone metastases. Experience with spinal SRS has increased clinical practitioners' confidence, and prescription doses have increased from 12 Gy to 16 Gy with reports of up to 24 Gy. As doses have escalated, the dose limiting toxicity of the vertebral bodies themselves has become a concern. One experienced group has reported approximately a 39% rate of progressive vertebral fracture following spinal radiosurgery to 24 Gy. [4], [10].

The long term effects of high-dose irradiation on bone strength are not well-known. Rissanen et al. reported the results of single-dose radiation on bone turnover in the humerus and femurs of dogs with 5 Gy, 10 Gy, or 40 Gy at four days, two weeks, or two months [11], [12]. It was observed that bone spaces had poor cellularity as little as four days after 5 Gy and osteocytes appeared to be radio-resistant up to 40 Gy in the early phase. Similar results persisted at the two week assessment but were accompanied by poorly mineralized areas. At two months, new bone formation was observed but many trabeculae were acellular and thrombosed blood vessels were seen in both the 10 and 40 Gy groups. Followup ended after two months so it is unknown whether new bone formation continued or if blood vessels continued to sclerose resulting in further morbidity. Significant research has been done regarding the radiation sensitivity of the bone marrow, showing that low doses of radiation deplete the marrow of its hematopoietic potential, persisting over time with fatty marrow replacement [13], [14]. Developing an accurate, non-invasive method to ascertain the biomechanical properties of bone would allow future study of the ramifications of high dose SRS treatments on patients.

Ultrasound velocity in solids is deterministically related to the mechanical stiffness (elastic modulus) of the material, a relationship that has been experimentally validated for bone [15]–[19]. In contrast to materials such as metals, bone material elastic modulus and ultimate strength are positively related [20]–[23]. Thus, non-invasive approaches based on ultrasound

J.E. Pollard, J. Steinmann-Hermsen and E. Richer are with the Department of Mechanical Engineering, SMU, Dallas, TX 75205, USA; e-mail: richer@lyle.smu.edu.

P. Medin is with the Department of Radiation Oncology, UT Southwestern Medical Center at Dallas, Dallas, TX 75390, USA

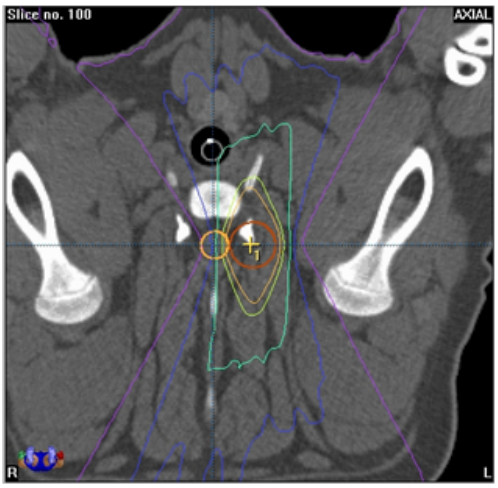

Fig. 1. Axial view of the irradiated area with the green isoline displaying the nominal dose distribution.

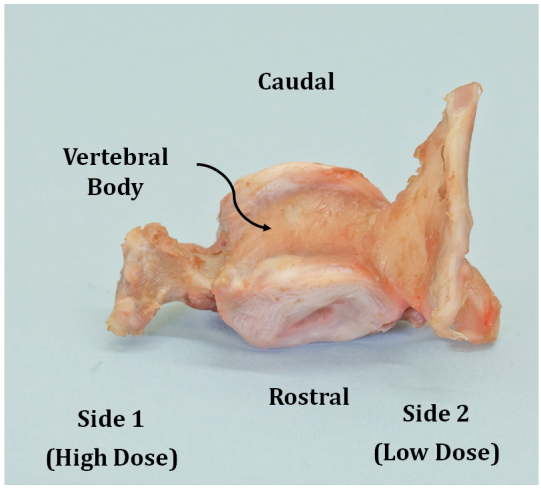

Fig. 2. Pictured is an actual vertebra, radiated at 16 Gy on half of the vertebral body. It is evident that at this prescribed dose, the radiation therapy distorts the bone life cycle.

have been proposed to assess bone strength by measuring ultrasound velocity both *in vitro* [21], [22] and *in vivo* [17].

Yucatan minipigs served as the *in vitro* biological model because of their physiological similarities to humans. Due to vertical posture, the human spine is predominantly loaded by axial compression, resulting in a vertebral bone microstructure oriented from endplate to endplate [24]. While quadruped spines may be subjected to additional loads, the musculature that controls posture and movement is structured such that axial compression is also the dominant force, as demonstrated by the axial orientation of trabeculae in their vertebrae [25]. Porcine cervical vertebrae are of similar size to their human counterparts, making this animal model appropriate for studying the effects of spinal SRS.

Determining the ultrasound propagation velocity in irradiated vertebral bodies could serve as a good indicator of the strength of bone, especially if comparative measurements in non-irradiated vertebrae are obtained. This information could be used to determine the highest safe dose for spinal SRS in a non-destructive, non-invasive manner.

II. Materials and Methods

A. Porcine Model

Spinal Stereotactic Radiosurgery was performed on four Yucatan Minipigs using a *Novalis* Linear Accelerator (BrainLAB AG, Feldkirchen, Germany) [26]. The irradiated cylindrical volume, about 5 cm in length and 2 cm in diameter, was focused on half of the fourth to the seventh cervical vertebra. The target area was positioned lateral to the cervical spinal cord resulting in a dose distribution with the 90%, 50%, and 10% isodose lines , as shown in Fig.1. Pigs A and B were administered a dose of 16 Gy while Pigs C and D were given 18 Gy. This study conformed to all national and local regulations regarding the use of animals for research and was approved by the institutional Animal Care and Use Committee at the University of Texas - Southwestern Medical Center (UTSWMC). The locomotion abilities and neurological response of the swine were observed for a minimum of 12 months to determine the radiation effects on the spinal cord. At the conclusion [26], [27], the animals were euthanized and the cervical vertebrae were removed, imaged using micro x-ray Computed Tomography (μCT), and stored in a 0.9% saline solution.

The cervical segment of the spines of all animals presented obvious asymmetry: the transverse processes on the high dose side were noticeably smaller than the ones on the low dose side (see Fig. 2). Moreover, the irradiated side of the vertebral bodies was significantly shorter in the axial direction.

Each vertebral body was cut into two 5x6x7 mm parallelepipedic samples, distributed symmetric about the middle plane, using a slow speed bone saw (Buehler Isomet Low Speed). Consistent alignment of the dimension of the samples with the anatomical directions of the vertebrae allowed easy directional identification during measurements. The samples were stored in individual acrylic containers at -20°C in a 0.9% saline solution [28].For each vertebra two samples were obtained, separating the high dose (side 1) and the low dose (side 2) irradiation zones. Control samples from the non-irradiated cervical vertebrae were obtained in a similar way. The bone marrow was not removed since the goal of the research was to assess the properties of the bone as close to its normal state as possible. The trabecular bone samples were measured, weighed, and the apparent densities calculated prior to ultrasound measurements.

B. Experimental Setup and Frequency Optimization

The experimental setup used to acquire all the ultrasound data included a high voltage narrow pulse generator and amplifier (model 5072PR, Olympus NDT Inc., Waltham, MA), pairs of frequency matched ultrasound transducers (Olympus NDT Inc.), a high speed signal digitizer (NI Scope Card USB-5133, National Instruments, Austin, TX) with a sampling rate of 100MS/s and 12-bit resolution, and custom data acquisition software written in LABview v8.2 (National Instruments, Austin, TX). As seen in the setup diagram, Fig. 3,

the transducers were arranged in a traditional transmission measurement positions. Ultrasound gel or water immersion were used as coupling agents. Ultrasound measurements were

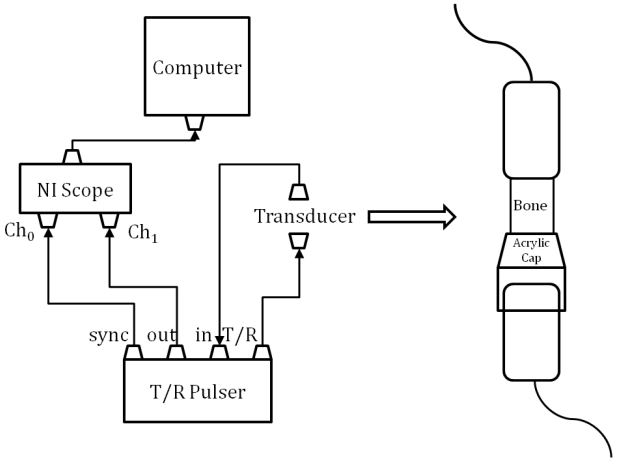

Fig. 3. Diagram of the experimental setup used for ultrasound propagation velocity measurements.

conducted at several frequencies in the axial and the transverse directions of the samples.

The majority of research papers that report ultrasound velocity measurements in trabecular bone used relatively low frequency transducers (50 kHz to 500 kHz) [19], [29], [30]. However, porcine vertebra are small in comparison to the more commonly used bovine femur. Accordingly, the samples of trabecular bone that can be obtained from the vertebral bodies are much smaller, comparable in dimension with the wave length of the ultrasonic signal. Thus, the propagation velocity of the ultrasound signal can be uncertain since bar velocity (v_{bar}) occurs when the entire specimen is excited by the transmitting ultrasound wave, while bulk velocity (v_{bulk}) occurs when the cross-section of the specimen is much larger than the wavelength (the wave does not perceive the solid's boundaries). The bar and bulk velocities relate with the mechanical properties of the bone as follows:

$$v_{bar} = \sqrt{\frac{E}{\rho}} \quad (1)$$

$$v_{bulk} = \sqrt{\frac{\kappa}{\rho}} \quad (2)$$

where E is the Young's Modulus (Pa), ρ is the apparent density (kg/m^3), $\kappa = \frac{E}{3(1-2\nu)}$ is the bulk modulus, and ν is Poisson's ratio (typically between 0.2 to 0.3) [19]. The lower frequencies commonly used in bovine trabecular bone samples have wavelengths that were larger then our sample size.

In order to determine the optimum ultrasound frequency for the available sample size, 5x6x7 mm parallelepipedic samples from materials with known speed of sound (Acrylic, Bacon-P58, Black Nylon, Delrin, Teflon, White Nylon) were tested using transducers ranging from 50 kHz up to 5 MHz. Velocity of ultrasound propagation was calculated as [31],

$$v = \frac{c_w}{1 + \frac{c_w \Delta t}{l}} \quad (3)$$

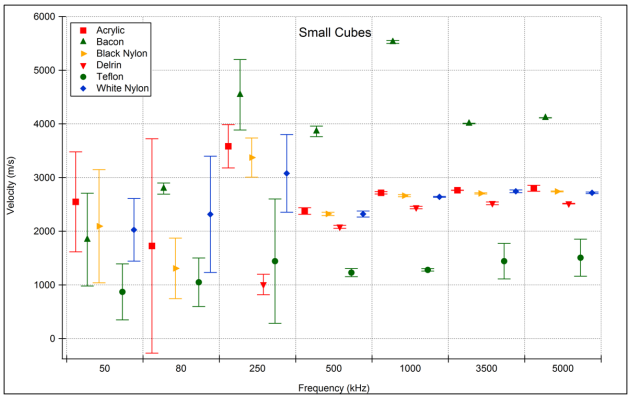

Fig. 4. Propagation velocity and measurement errors in small samples using ultrasound frequencies from 50 kHz to 5 MHz.

where c_w is the acoustic velocity in water, Δt is the difference in transit time of an ultrasound pulse transmitted through the cube, and l is the cube thickness. The results showed that, for the sample size obtainable from the vertebrae, the best measurement accuracy is obtained for frequencies above 1 MHz (see Fig. 4).

C. Velocity Measurements

The digitized ultrasound signals (see Fig. 5, solid line) were imported into a custom analysis software developed in the Igor Pro 6.03A (WaveMetrics, Inc., Lake Oswego, OR) programming environment.

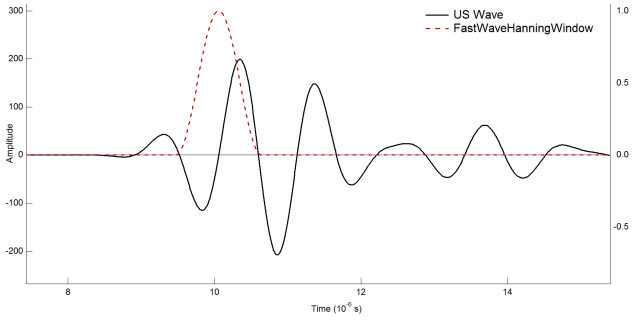

Fig. 5. Transmitted ultrasound signal through vertebral trabecular bone. Note the interference and the slight change of the frequency around 12.5 μs.

The velocity was calculated two ways: a traditional method based on the time–of–flight (TOF) collected from the first signal departure from the zero axis, and a method based on the short time Fourier transform (STFT) of the signal. The STFT of a signal $s(t)$ is defined as [32],

$$G_{\phi S}(b,\omega) = \int_{-\infty}^{\infty} s(t)\phi_{b,\omega}(t)dt \quad (4)$$

$$\phi b,\omega(t) = \phi(t-b)e^{-j\omega t} \quad (5)$$

where ω is the angular frequency and $\phi(t)$ is a window function,

$$\phi(t) = \begin{cases} \phi_t, & \tau[b-\tau, b+\tau] \\ 0, & \text{otherwise} \end{cases} \quad (6)$$

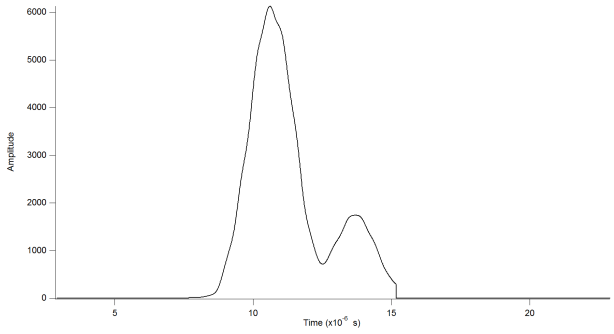

Fig. 6. Plot of the STFT amplitude versus the moment in time for the ultrasound signal transmitted through the vertebral bone. The two peaks correspond to the "in phase" and "out of phase" waves predicted by Biot's model

where b is the moment in time, and τ is the time window width. Eqs. (4)–(6) show that by truncating the signal $s(t)$ with a window of width 2τ, one can evaluate the energy distribution at the specified moment b. While any truncating window wider than the wavelength would work, a Hanning time window function was selected for its smoothing properties (see Fig. 5, dashed line). Recording the amplitude of a selected frequency component in the spectrum of the signal as the moment in time is varied, the propagation information of the specific frequency component is obtained. Thus, the ultrasound propagation time can be obtained from the position of the peak in the STFT time plot (see Fig. 6). The presence of two peaks in the amplitude plot suggests that there are two distinct waves arriving at different moments in time. Indeed, trabecular bone is in essence a biphasic material, made of a solid (bone) and a fluid (marrow) [30]. In 1956 Biot proposed a model for porous media in which the ultrasound energy propagates in two waves at different velocities [33]–[36]. One of the waves occurs when the solid and liquid are pulsing in phase and the other wave occurs when the materials are pulsing out of phase. If the frequency of the ultrasound signal is sufficiently large, above 1 MHz for the dimensions of our samples, a reasonable separation of the "fast wave" from the "slow wave" will occur as seen in Fig. 5. Thus, two peaks will be present in the STFT, allowing both velocities to be estimated.

After the propagation velocity was measured using the TOF and STFT methods, Eq. (1) can be used to estimate Young's Modulus (E):

$$E = \rho v_i^2 \tag{7}$$

where ρ is the apparent density and v_i is the calculated velocity of ultrasound in the i^{th} direction.

III. Results and Discussion

The ultrasound propagation velocity through the trabecular bone samples was obtained for the high dose (side 1) and low dose (side 2) irradiated vertebrae, as well as for control samples (side 1, and side 2) from adjacent non-radiated vertebrae. Since the control vertebrae were not irradiated there was no reason to expect a difference between the two sides. The measurement for the two sides of the control vertebrae were kept separate to gain insight into the natural variability of the measured velocity. Unfortunately, the small number of available animals ($N = 4$) prevented a relevant statistical analysis.

TABLE I
Percent Difference of E between side 1 and side 2

	Control	Radiated
Fast Wave	4.3%	9.8%
Slow Wave	14.7%	38.1%

Both methods detailed in the previous section, TOF and STFT, were used. While the two methods produced different absolute values, as expected, both show the same behavior when the results for the side 1 and side 2 irradiated samples were compared. As seen in Fig. 7, the largest difference between the velocities of side 1 (high dose) and side 2 (low dose) of the irradiated vertebrae was observed in the axial direction when the fast wave was used. The high dose side consistently showed a lower velocity. In the transverse direction the difference between the two sides was less pronounced but exhibited the same trend. The results obtained using the slow wave velocity, Fig. 8, show a similar behavior for both the axial and transverse directions, but the standard deviation is significantly larger.

No consistent difference was observed between the ultrasound velocity for samples obtained from irradiated and control vertebrae. Often the ultrasound velocity for the control samples was lower than for the corresponding irradiated samples, suggesting that adjacent non-irradiated vertebra are not effective controls.

Selecting a proper ultrasound frequency in relation to the sample size and wavelength was shown to be important to achieve minimum measurement errors as well as the separation of a fast and slow wave. One unexpected observation, since it is not predicted by the Biot's model, was that the frequency of the fast wave was larger than the frequency of the slow wave, especially in the transverse direction. We are not aware of any other research article reporting this observation.

The Young's Modulus E, calculated using Eq. 7 for all the samples, is shown Figures 9b and 9a. While both the irradiated and control samples show the same tendency of lower E for side 1, the relative difference between side 1 and side 2 for the irradiated vertebrae is greater than the difference of side 1 and side 2 for the control when all samples are considered. The results are shown in Table I.

Ultrasound propagation velocity through irradiated vertebral bone samples was observed to be dose dependent, decreasing with increasing dose. The dose-velocity relationship was more apparent in the axial direction and for fast wave velocity. This result was consistent when the Young's modulus was estimated using the ultrasound velocity and the apparent density.

Comparison of propagation velocity through irradiated samples versus adjacent but non-irradiated vertebrae proved unreliable. This finding may be due to variability in the mechanical loads pres ented to individual vertebra throughout the cervical spine. This implies that, in clinical practice, a measurement obtained prior to the SRS at the treatment location should be used as baseline for data analysis.

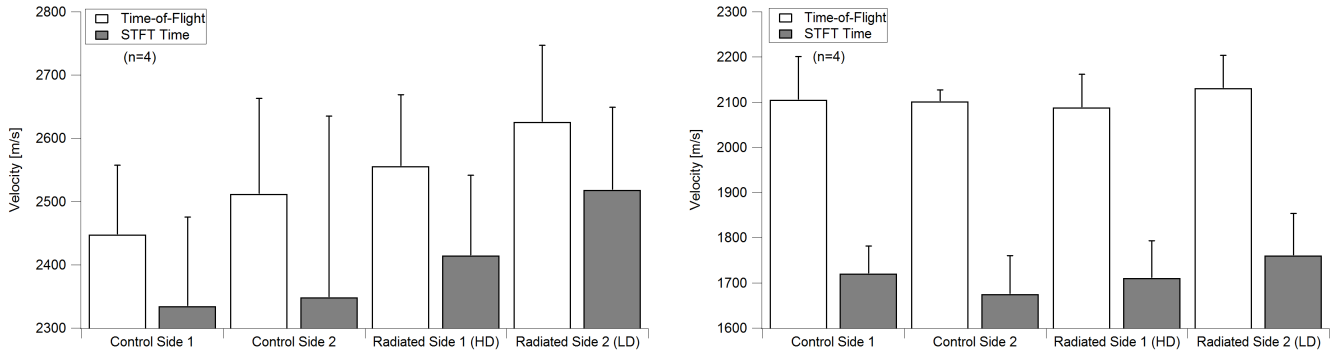

(a) (b)

Fig. 7. Average ultrasound velocity for the irradiated and control vertebrae measured in the axial (a) and transverse (b) directions using the TOF and the STFT peak for the fast wave

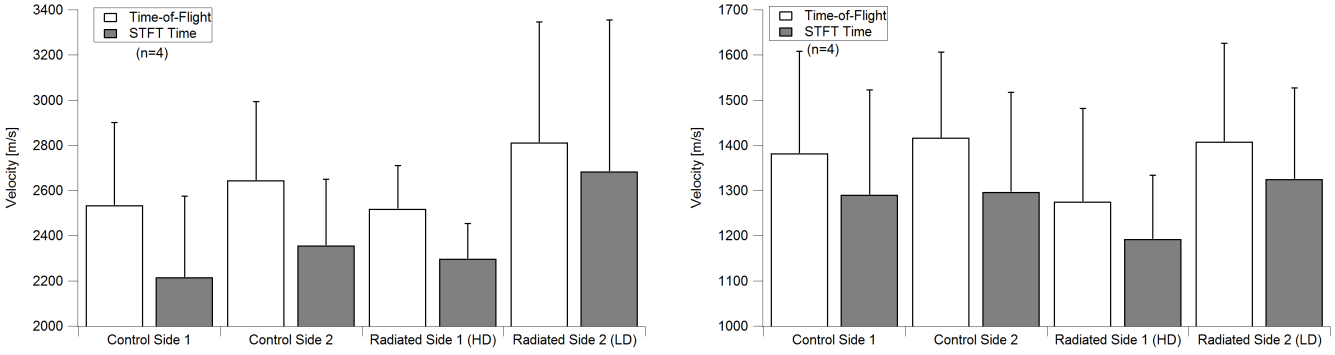

(a) (b)

Fig. 8. Average ultrasound velocity for the irradiated and control vertebrae measured in the axial (a) and transverse (b) directions using the TOF and the STFT peak for the slow wave

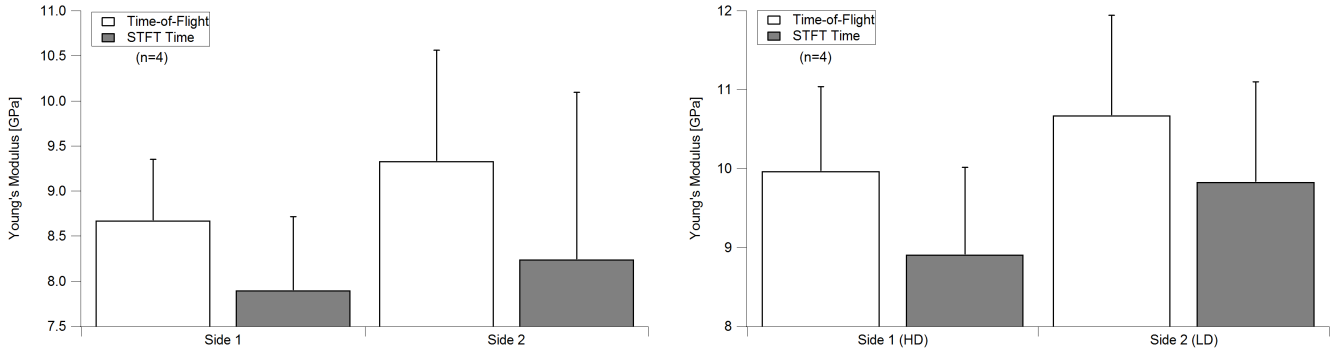

(a) (b)

Fig. 9. The Young's Modulus for the control vertebrae (a) and the radiated vertebrae (b).

ACKNOWLEDGMENT

This work was partially supported by NIH R01-049517 grant, and by a startup grant form Bobby B. Lyle School of Engineering, SMU, Dallas, TX.

REFERENCES

[1] P. Black, "Spinal metastasis: current status and recommended guidelines for management," *Nurosurgery*, vol. 5, no. 6, pp. 726–746, 1979.

[2] T. N. Byrne and S. G. Waxman, *Spinal cord compression: Diagnosis and principles of management*. F.A. Davis (Philadelphia), 1990, iSBN 0803614659.

[3] P. C. Gerszten, S. A. Burton, C. Ozhasoglu, and W. C. Welch, "Radiosurgery for spinal metastases: clinical experience in 500 cases from a single institution." *Spine (Phila Pa 1976)*, vol. 32, no. 2, pp. 193–199, Jan 2007. [Online]. Available: http://dx.doi.org/10.1097/01.brs.0000251863.76595.a2

[4] Y. Yamada, M. H. Bilsky, D. M. Lovelock, E. S. Venkatraman, S. Toner, J. Johnson, J. Zatcky, M. J. Zelefsky, and Z. Fuks, "High-dose, single-fraction image-guided intensity-modulated radiotherapy for metastatic spinal lesions," *International Journal of Radiation Oncology*Biology*Physics*, vol. 71, no. 2, pp. 484 – 490, 2008. [Online]. Available: http://www.sciencedirect.com/science/article/B6T7X-4RPVHYX-M/2/67b77afe8de1166e15f8ba6a06065b1f

[5] R. A. Patchell, P. A. Tibbs, W. F. Regine, R. Payne, S. Saris, R. J. Kryscio, M. Mohiuddin, and B. Young, "Direct decompressive surgical resection in the treatment of spinal cord compression caused by metastatic cancer: a randomised trial." *Lancet*, vol. 366, no. 9486, pp. 643–648, 2005. [Online]. Available: http://dx.doi.org/10.1016/S0140-6736(05)66954-1

[6] A. Jemal, R. Siegel, E. Ward, Y. Hao, J. Xu, T. Murray, and M. J. Thun, "Cancer statistics, 2008," *CA Cancer J Clin*, vol. 58, no. 2, pp. 71–96, 2008. [Online]. Available: http://caonline.amcancersoc.org/cgi/content/abstract/58/2/71

[7] R. G. Parker and H. C. Berry, "Late effects of therapeutic irradiation on the skeleton and bone marrow," *Cancer*, vol. 37, no. S2, pp. 1162–1171, February 1975.

[8] F. B. Zimmermann, H. Geinitz, S. Schill, A. Grosu, U. Schratzenstaller, M. Molls, and B. Jeremic, "Stereotactic hypofractionated radiation therapy for stage i non-small cell lung cancer." *Lung Cancer*, vol. 48, no. 1, pp. 107–114, Apr 2005. [Online]. Available: http://dx.doi.org/10.1016/j.lungcan.2004.10.015

[9] P. Fritz, H.-J. Kraus, T. Blaschke, W. Mhlnickel, K. Strauch, W. Engel-Riedel, A. Chemaissani, and E. Stoelben, "Stereotactic, high single-dose irradiation of stage i non-small cell lung cancer (nsclc) using four-dimensional ct scans for treatment planning." *Lung Cancer*, vol. 60, no. 2, pp. 193–199, May 2008. [Online]. Available: http://dx.doi.org/10.1016/j.lungcan.2007.10.005

[10] P. S. Rose, I. Laufer, P. J. Boland, A. Hanover, M. H. Bilsky, J. Yamada, and E. Lis, "Risk of fracture after single fraction image-guided intensity-modulated radiation therapy to spinal metastases." *Journal Of Clinical Oncology: Official Journal Of The American Society Of Clinical Oncology*, vol. 27, no. 30, pp. 5075 – 5079, 2009.

[11] P. Rissanen, P. Rokkanen, and S. Paatsama, "The effect of co60 irradiation on bone in dogs. i. mature bone." *Strahlentherapie*, vol. 137, no. 2, pp. 162–169, Feb 1969.

[12] ——, "The effect of co60 irradiation of bone in dogs. ii. growing bone." *Strahlentherapie*, vol. 137, no. 3, pp. 344–354, Mar 1969.

[13] L. K. Mell, H. Tiryaki, K.-H. Ahn, A. J. Mundt, J. C. Roeske, and B. Aydogan, "Dosimetric comparison of bone marrow-sparing intensity-modulated radiotherapy versus conventional techniques for treatment of cervical cancer," *International Journal of Radiation Oncology*Biology*Physics*, vol. 71, no. 5, pp. 1504 – 1510, 2008. [Online]. Available: http://www.sciencedirect.com/science/article/B6T7X-4T14Y64-6/2/03fb1187a7741c5fc4dd4a1a483d8c81

[14] E. J. Hall, M. Marchese, T. K. Hei, and M. Zaider, "Radiation response characteristics of human cells in vitro." *Radiat Res*, vol. 114, no. 3, pp. 415–424, Jun 1988.

[15] F. Cavani, G. Giavaresi, M. Fini, L. Bertoni, F. de Terlizzi, R. Barkmann, and V. Cane, "Influence of density, elasticity, and structure on ultrasound transmission through trabecular bone cylinders," *IEEE Transactions on Ultrasonics, Ferroelectrics, and Frequency Control*, vol. 55, no. 7, pp. 1465–1472, 2008.

[16] C.-C. Gler, "Quantitative ultrasound–it is time to focus research efforts," *Bone*, vol. 40, no. 1, pp. 9 – 13, 2007. [Online]. Available: http://www.sciencedirect.com/science/article/B6T4Y-4KSSWF7-4/2/a0887b701babda426972288bea63dd4c

[17] E. Richer, M. A. Lewis, C. V. Odvina, M. A. Vazquez, B. J. Smith, R. D. Peterson, J. R. Poindexter, P. P. Antich, and C. Y. C. Pak, "Reduction in normalized bone elasticity following long-term bisphosphonate treatment as measured by ultrasound critical angle reflectometry." *Osteoporos Int*, vol. 16, no. 11, pp. 1384–1392, Nov 2005. [Online]. Available: http://dx.doi.org/10.1007/s00198-005-1848-x

[18] D. Hans, M. E. Arlot, A. M. Schott, J. P. Roux, P. O. Kotzki, and P. J. Meunier, "Do ultrasound measurements on the os calcis reflect more the bone microarchitecture than the bone mass?: A two-dimensional histomorphometric study," *Bone*, vol. 16, no. 3, pp. 295 – 300, 1995. [Online]. Available: http://www.sciencedirect.com/science/article/B6T4Y-3Y6HHP4-4V/2/e02b9cb7daf2dffc24eaae95f5728b38

[19] Y. H. An and R. A. Draughn, *Mechanical Testing of Bone and the BoneImplant Interface*. CRC Press (Boca Raton), 2000.

[20] H. G. Abendschein W, "Ultrasonics and selected physical properties of bone." *Clin Orthop Relat Res.*, vol. 69, pp. 294–301, Mar-Apr 1970.

[21] P. P. Antich, J. A. Anderson, R. B. Ashman, J. E. Dowdey, J. Gonzales, R. C. Murry, J. E. Zerwekh, and C. Y. C. Pak, "Measurement of mechanical properties of bone material in vitro by ultrasound reflection: Methodology and comparison with ultrasound transmission," *Journal of Bone and Mineral Research*, vol. 6, no. 4, pp. 417–426, 1991. [Online]. Available: http://dx.doi.org/10.1002/jbmr.5650060414

[22] S. S. Mehta, P. P. Antich, M. M. Daphtary, D. G. Bronson, and E. Richer, "Bone material ultrasound velocity is predictive of whole bone strength," *Ultrasound in Medicine & Biology*, vol. 27, no. 6, pp. 861 – 867, 2001. [Online]. Available: http://www.sciencedirect.com/science/article/B6TD2-438BW6D-H/2/0a4973a8d9c353fa369e73dc9d749738

[23] J. Y. Rho, R. B. Ashman, and C. H. Turner, "Young's modulus of trabecular and cortical bone material: Ultrasonic and microtensile measurements," *Journal of Biomechanics*, vol. 26, no. 2, pp. 111 – 119, 1993. [Online]. Available: http://www.sciencedirect.com/science/article/B6T82-4BYSH8F-RF/2/278e95a3c1a1d00c6ce76a173dd4c2d2

[24] T. H. Smit, A. Odgaard, and E. Schneider, "Structure and function of vertebral trabecular bone." *Spine (Phila Pa 1976)*, vol. 22, no. 24, pp. 2823–2833, Dec 1997.

[25] T. Smit, "The use of a quadruped as an in vivo model for the study of the spine - biomechanical considerations," *European Spine Journal*, vol. 11, pp. 137–144, 2002, 10.1007/s005860100346. [Online]. Available: http://dx.doi.org/10.1007/s005860100346

[26] P. M. Medin, R. D. Foster, A. J. van der Kogel, J. W. Sayre, W. H. McBride, and T. D. Solberg, "Spinal cord tolerance to single-fraction partial-volume irradiation: a swine model." *Int J Radiat Oncol Biol Phys*, vol. 79, no. 1, pp. 226–232, Jan 2011. [Online]. Available: http://dx.doi.org/10.1016/j.ijrobp.2010.07.1979

[27] P. M. Medin, T. D. Solberg, A. A. F. D. Salles, C. H. Cagnon, M. T. Selch, J. P. Johnson, J. B. Smathers, and E. R. Cosman, "Investigations of a minimally invasive method for treatment of spinal malignancies with linac stereotactic radiation therapy: accuracy and animal studies." *Int J Radiat Oncol Biol Phys*, vol. 52, no. 4, pp. 1111–1122, Mar 2002.

[28] M. Laursen, F. Christensen, C. Bnger, and M. Lind, "Optimal handling of fresh cancellous bone graft different peroperative storing techniques evaluated by in vitro osteoblast-like cell metabolism," *Acta Orthopaedica*, vol. 74, no. 4, pp. 490–496, 2003. [Online]. Available: http://informahealthcare.com/doi/abs/10.1080/00016470310017848

[29] G. Renaud, S. Calle, J.-P. Remenieras, and M. Defontaine, "Exploration of trabecular bone nonlinear elasticity using time-of-flight modulation," *IEEE Transactions on Ultrasonics, Ferroelectrics, and Frequency Control*, vol. 55, no. 7, pp. 1497–1507.

[30] P. Nicholson, "Ultrasound and the biomechanical competence of bone," *Ultrasonics, Ferroelectrics and Frequency Control, IEEE Transactions on*, vol. 55, no. 7, pp. 1539 –1545, 2008.

[31] J. E. Pollard, "The optimization of ultrasound measurement methodology for the detection of the effect of radiation on porcine vertebrae," Master's thesis, Southern Methodist University, December 2009.

[32] B. Zhao, O. A. Basir, and G. S. Mittal, "Estimation of ultrasound attenuation and dispersion using short time fourier transform." *Ultrasonics*, vol. 43, no. 5, pp. 375–381, Mar 2005. [Online]. Available: http://dx.doi.org/10.1016/j.ultras.2004.08.001

[33] M. A. Biot, "Theory of propagation of elastic waves in a fluid-saturated porous solid. i. low-frequency range," *The Journal of the Acoustical*

Society of America, vol. 28, no. 2, pp. 168–178, 1956. [Online]. Available: http://link.aip.org/link/?JAS/28/168/1

[34] ——, "Theory of propagation of elastic waves in a fluid-saturated porous solid. ii. higher frequency range," *The Journal of the Acoustical Society of America*, vol. 28, no. 2, pp. 179–191, 1956. [Online]. Available: http://link.aip.org/link/?JAS/28/179/1

[35] Z. E. A. Fellah, N. Sebaa, M. Fellah, F. G. Mitri, E. Ogam, W. Lauriks, and C. Depollier, "Application of the biot model to ultrasound in bone: Direct problem," *IEEE Transactions on Ultrasonics, Ferroelectrics, and Frequency Control*, vol. 55, no. 7, pp. 1508–1515.

[36] N. Sebaa, Z. E. A. Fellah, M. Fellah, E. Ogam, F. G. Mitri, C. Depollier, and W. Lauriks, "Application of the biot model to ultrasound in bone: Inverse problem," *IEEE Transactions on Ultrasonics, Ferroelectrics, and Frequency Control*, vol. 55, no. 7, pp. 1516–1523.